Characteristics and Microstructure of Geopolymer Mortars incorporating Ground Granulated Blast Furnace Slag and Calcined Dolomite Powder: A Sustainable Solution for Construction Materials

Mostafa Shaaban
Civil Engineering Department, Giza Engineering Institute, Egypt
mostafa.shaaban@gei.edu.eg (corresponding author)

Omnia Farouk Hussien
Faculty of Engineering, Egyptian Russian University, Egypt
omniafarouk@eru.edu.eg

Safinaz Khalifa
Faculty of Engineering, Egyptian Russian University, Egypt
safinaz-khalifa@eru.edu.eg

Received: 1 January 2025 | Revised: 26 January 2025 | Accepted: 31 January 2025

 DOI: https://doi.org/10.48084/etasr.10095

ABSTRACT

The global demand for environmentally sustainable and cost-effective materials that reduce carbon emissions and energy consumption has significantly risen. In this context, geopolymer binders, primarily sourced from industrial by-products or agricultural waste, have emerged as viable alternatives to traditional Ordinary Portland Cement (OPC). This study examines the characteristics and microstructure of two types of geopolymer mortars: one utilizing an alumina-rich binder, namely calcined clay, and the other employing a silica-rich binder, namely rice husk ash. Both mortar types incorporate a consistent 30% Ground Granulated Blast Furnace Slag (GGBFS), with Calcined Dolomite Powder (CDP) added in varying proportions of 10%, 15%, 20%, and 25%. A total of eight geopolymer mortar mixes, along with a reference mix consisting of 100% OPC, were prepared and evaluated for setting time, flowability, compressive strength, flexural strength, and dry density. Additionally, microstructural analysis was conducted using electron microscopy techniques. The results indicated that the clay-based geopolymer mortars outperformed those based on rice husk ash. Notably, the mixes containing 30% GGBFS, 50% calcined clay, and 20% calcined dolomite powder, as well as those with 30% GGBFS, 45% calcined clay, and 25% calcined dolomite powder, exhibited performance levels comparable to, or slightly exceeding, those of the reference mix.

Keywords-eco-friendly binder; sustainable materials; geopolymer binders; cement alternatives; recycled concrete aggregate; calcined dolomite powder

I. INTRODUCTION

Cement consumption has surged globally, with annual production having exeeded 4.7 billion tons in 2023, driven by the rapid pace of urbanization and infrastructure development [1]. Cement manufacturing is a significant source of environmental degradation, contributing to air pollution, resource depletion, and global climate change. The cement industry is responsible for approximately 7-8% of the global CO_2 emissions, primarily due to the calcination process and the combustion of fossil fuels for heat generation in kilns [2].

One of the major environmental impacts of cement manufacturing is greenhouse gas emissions. The calcination process releases CO_2 from limestone ($CaCO_3$) as it is converted to lime (CaO). Additionally, the use of fossil fuels to heat the kilns (at temperatures exceeding 1400°C) contributes further to the emission of CO_2, NO_x, and SO_2. Common fuels include coal, petroleum coke, and natural gas, all of which have high

carbon intensities. Resource depletion is another serious concern, as the production of cement requires vast amounts of raw materials, such as limestone, clay, and sand. These materials are often extracted through mining operations that disrupt landscapes, destroy habitats, and deplete non-renewable resources. Water is also consumed in large quantities, putting additional strain on local water supplies [3]. In addition to greenhouse gases, cement manufacturing produces particulate matter during quarrying, grinding, and kiln operation. These fine dust particles can become airborne, leading to air pollution and posing health risks. The workers at cement plants and nearby communities are particularly vulnerable to these health effects.

Waste generation in the form of kiln dust, clinker dust, and other process residues presents another environmental challenge. These waste products often contain harmful substances, like heavy metals, which can leach into soil and groundwater if not properly managed, leading to potential contamination and long-term environmental damage [4].

Cement production is highly energy-intensive, consuming around 3-4 gigajoules (GJ) of energy per ton of cement produced. This large energy demand exacerbates global energy consumption and increases reliance on fossil fuels, contributing further to environmental stress and carbon emissions [5].

Given the significant environmental impact of the cement industry, there is an urgent need to explore a sustainable alternative to traditional Portland cement. One promising avenue is the development of alternative binders, such as geopolymers. Geopolymer binders provide significant environmental advantages due to their lower CO_2 emissions by up to 80% compared to traditional Portland cement. Geopolymer binders also facilitate the recycling of industrial waste, such as Fly Ash (FA) from coal combustion and slag from steel production, thereby reducing the need for virgin raw materials and diverting waste from landfills [6]. Additionally, the production of geopolymers requires less energy, further reducing greenhouse gas emissions [7].

Several studies have explored the use of Granulated Blast Furnace Slag (GBFS) in the preparation of geopolymers. GBFS is a byproduct of the steel industry, rich in calcium and contains significant amounts of SiO_2 and Al_2O_3, making it effective in activating geopolymerization and improving the mechanical properties of geopolymers [8]. Incorporating GBFS and FA-based geopolymer can increase the strength and reduce the time of setting [9]. Additionally, utilizing GBFS and red mud to prepare geopolymers can achieve a maximum 28-day compressive strength of 65.7 MPa with a GBFS to red mud ratio of 1:1 [10]. Including 40% GBFS content in geopolymers produced from coal gangue can significantly enhance compressive strength, with increases of up to 59.08% [11].

Calcium oxide (CaO), commonly derived from limestone, provides an alkaline environment necessary for geopolymerization. Adding CaO to geopolymer binders improves compressive strength and accelerates setting time. While CaO production involves CO_2 emissions, its use in geopolymers can still result in a net reduction of environmental impact compared to traditional cement production.

Rice husk ash (RHA), rich in amorphous silica, is a by-product of rice milling. Using RHA in geopolymers aids in waste management and reduces the environmental footprint. RHA-based geopolymers exhibit excellent mechanical properties due to the high reactivity of RHA silica, which accelerates setting and hardening [12]. Additionally, RHA geopolymers can reduce CO_2 emissions and energy consumption compared to conventional cement [13]. The addition of 1%, 1.5%, and 2% of rice husk fibers and 5% of paper ash has increased the flexural strength of RHA-based geopolymer mortar [14].

Calcined clay-based geopolymer binders represent a promising advancement in sustainable construction materials. With enhanced mechanical properties, durability, and thermal stability, coupled with a reduced environmental impact compared to traditional Portland cement, these geopolymers offer significant benefits. Ongoing research into optimizing mix designs, activation methods, and applications continues to advance the development of calcined clay-based geopolymers, supporting their potential to transform the construction industry. Recent studies have reported that geopolymers incorporating metakaolin achieve compressive strengths ranging from 50 MPa to 70 MPa, depending on the mix design and curing conditions.

The durability of calcined clay-based geopolymers is a key factor in their viability as a construction material. Research has demonstrated that these geopolymers exhibit excellent resistance to environmental stresses, including sulfate and chloride attacks, freeze-thaw cycles, and elevated temperatures. Calcined clay-based geopolymers maintain their structural integrity and performance under severe environmental conditions, highlighting their potential for use in challenging environments. Additionally, calcined clay-based geopolymers retain their mechanical properties and structural stability at temperatures up to 800°C, making them suitable for applications requiring high thermal resistance. One of the primary advantages of calcined clay-based geopolymers is their reduced environmental impact compared to traditional Portland cement. The production of calcined clay requires lower temperatures than the calcination of limestone for cement, resulting in lower CO_2 emissions. Calcined clay-based geopolymers can reduce CO_2 emissions by up to 50% compared to conventional cement.

Previous studies prove that increasing the calcium ion (Ca^{2+}) content in raw materials has been shown to enhance the early strength of geopolymers [15, 16]. The early strength development of geopolymers is significantly influenced by curing methods [17, 18]. Traditional ambient curing techniques include standard curing, water curing, sealed curing, and dry curing [19-22]. However, recent studies have highlighted that alternative methods, such as heat curing and microwave curing, can substantially improve early strength. For instance, employing microwave curing for FA-based geopolymers can achieve compressive strengths exceeding 50 MPa after just 15 minutes of curing [23].

Recent studies have investigated the use of alternative alkaline activators and different activation conditions to enhance the performance of these materials. The combination

of sodium hydroxide and sodium silicate as activators significantly improves the setting time and strength development of calcined clay-based geopolymers [24].

A. Research Significance

The significance of this research lies in its potential to advance the development of geopolymer-based materials as a sustainable and high-performance alternative to traditional cement. As the construction industry faces increasing pressure to reduce its carbon footprint, geopolymers offer a promising solution due to their lower environmental impact, particularly in terms of CO_2 emissions during production. By investigating the role of key components, like silicon dioxide (SiO_2) and aluminum oxide (Al_2O_3), in optimizing the mechanical properties and microstructure of geopolymers, this study aims to unlock new possibilities for enhancing the performance of geopolymer mortar in various applications, from structural components to high-performance infrastructure. Understanding the interaction between these materials at a molecular level can provide insights into the geopolymerization process, enabling better control over properties. Ultimately, the findings of this research could contribute to the wider adoption of geopolymers in sustainable construction practices, offering a viable solution for building more durable, cost-effective, and environmentally friendly structures.

II. MATERIALS AND EXPERIMENTAL PROCEDURE

A. Materials

To conduct the experimental study, various materials were employed, including different types of fine aggregates and cementitious materials. Natural sand, with a fineness modulus of 2.9 and a bulk density of 1495 kg/m^3, meeting the guidelines of [25], was used as the fine aggregate in the control mix, as depicted in Figure 1(a).

For the geopolymer mortars, Recycled Concrete Aggregate (RCA) with a fineness modulus of 3.2 and a bulk density of 1410 kg/m^3 was utilized as fine aggregate. RCA, produced from crushed concrete by laboratory ball mill, serves as a sustainable alternative to natural fine aggregates in geopolymer mortars, as shown in Figure 1(b). Using RCA reduces the need for virgin materials and minimizes waste, supporting sustainability goals.

Fig. 1. The two used fine aggregates.

Table I presents the properties of the two used fine aggregates in sample preparation, while Figure 2 shows the particle size distribution of these aggregates.

TABLE I. PROPERTIES OF FINE AGGREGATES

Property	Fine RCA	Natural sand
Specific gravity	2.23	2.58
Volume density	1410	1495
Water absorption (%)	5.67	1.9
Los Angeles abrasion (%)	25.8	-
Crushing Value (%)	28.4	-

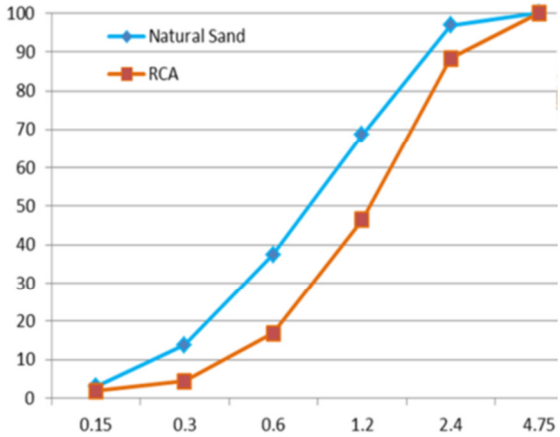

Fig. 2. Grading curve of used fine aggregates.

OPC CEM I 42.5 Type N, conforming to [26], was used as the binder in the reference mix. In the geopolymer mortar mixes, cement was entirely substituted with alternative cementitious materials, as illustrated in Figure 3. These included GGBFS with a specific gravity of 2.9, RHA with a specific gravity of 2.1, calcined clay, and calcined dolomite powder, with specific gravities of 2.6 and 2.2, respectively.

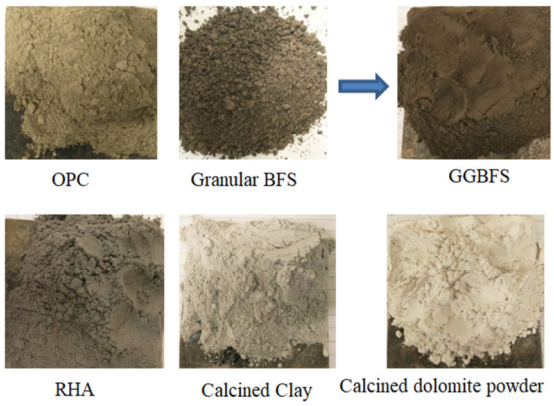

Fig. 3. Cementitious materials utilized in mortar mixtures.

GGBFS was supplied by Ezz steel company-Egypt, and grounded by a laboratory ball mill. RHA was obtained from the combustion of rice husk, the protective outer covering of rice grains. The production process involved burning rice husks under controlled conditions, having resulted in ash grounded by a laboratory ball mill to the powder size. Calcined clay and CDP were supplied by Nourmetec Company for Refractory Products- Egypt.

Table II presents the physical properties and chemical compositions of the cementitious materials used, while, Figure 4 portrays their particle size distributions.

TABLE II. PHYSICAL PROPERTIES AND CHEMICAL COMPOSITIONS OF CEMENTITIOUS MATERIALS

Material	Cao	SiO_2	Al_2O_3	Fe_2O_3	MgO	K_2O
OPC	58.1	25.5	7.37	4.16	1.76	0.7
GGBFS	40.42	32.22	15.0	0.5	7.4	0.47
RHA	1.1	89.9	0.45	0.47	0.8	3.2
Clay	0.84	54.7	37.4	1.72	0.42	-
CDP	50.6	15.3	1.25	1.0	27	0.15
Particle size						
D-value%	OPC	GGBFS	RHA	Clay	CDP	
D10	1.1	0.4	1.7	0.3	1.6	
D50	9.9	1.75	14.7	1.5	13.9	
D90	22.6	3.86	31.5	3.5	29.4	

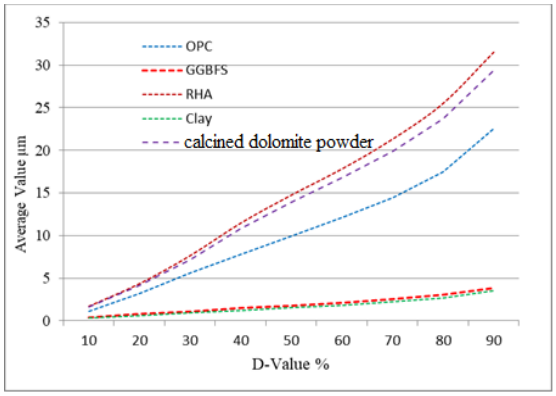

Fig. 4. Particle size distribution of used binders.

Sodium hydroxide (NaOH) and sodium silicate (Na_2SiO_3) solutions were utilized as alkali activators. Purified water was used to dissolve sodium hydroxide (NaOH) until the molarity reached 12. The alkali solution formed by mixing Na_2SiO_3 and NaOH solutions was prepared three hours before having been used. The potable water, which complies with [27], was utilized in the mixing of the dry materials. The water to binder (w/b) ratio was constant for all mixtures and equal to 0.4.

B. Mix Proportions and Preparation of Test Specimens

To assess the performance of the studied geopolymer binders as a fully cement alternative, nine mortar mixes were prepared. The standard mix ratio employed was a fine aggregate to binder ratio of 2:1, with a w/b ratio of 0.35, and an alkaline activator blended with the binders at a ratio of 0.44. The control mix, M0, contains 100% OPC and natural sand as fine aggregate.

The eight geopolymer mixes incorporated RCA as fine aggregate and a constant proportion of 30% GGBFS. These mixes included/were categorized into two groups. The first group, denoted by the symbol R, comprised four mixes with varying CDP percentages (10%, 15%, 20%, 25%), each combined with corresponding percentages of RHA (60%, 55%, 50%, 45%). The second group, identified by the symbol C, also consisted of four mixes with CDP percentages of 10%, 15%, 20%, 25%, but was/were blended with corresponding proportions of calcined clay (60%, 55%, 50%, 45%), as portrayed in Table III.

TABLE III. MIX DESIGNS OF MORTARS (kg/m^3)

Mix code	Mix designation	Fine aggregate		Cementitious materials					Water	NaOH sol	Sodium Silicate
		Sand	RCA	OPC	GGBFS	RHA	C. Clay	CDP			
M0	Control Mix	1495	-	500	-	-	-	-	200	-	-
M1	R60L10	-	1410	-	141	197	-	132	188	119	238
M2	R55L15	-		-		181	-	148			
M3	R50L20	-		-		164	-	165			
M4	R45L25	-		-		148	-	181			
M5	C60L10	-		-		-	197	132			
M6	C55L15	-		-		-	181	148			
M7	C50L20	-		-		-	164	165			
M8	C45L25	-		-		-	148	181			

The preparation process of each mortar was: Initially, the dry materials were placed in the mixer and stirred for 2 min. Then the alkali activator was poured into the mixer. Subsequently, water in prescribed proportions was added to obtain a homogenous mortar. The prepared fresh mortars were poured into standard molds, twenty-four hours after casting, as displayed in Figure 5. The specimens were, then, removed from the molds and stored at laboratory temperature, protected from water evaporation using plastic sheet.

To evaluate the new properties of the studied binders, the setting time test was conducted using a Vicat apparatus, following the guidelines of [28]. Also the fluidity of the mortar was assessed using the flow table test in accordance with [29].

Compressive strength, dry unit weight, flexural strength, and microstructure characterization tests were performed to evaluate the properties of the hardened mortars. These tests were conducted as follows:

- The dry unit weight was determined by measuring the mass and volume of the hardened mortar specimens dried by/in an oven, following the procedures outlined in [30].

- Compressive strength tests were conducted by subjecting 70 mm x 70 mm x 70 mm mortar cubes to uniaxial compression until failure, with the peak load having been recorded as the compressive strength, as per [31].
- Flexural strength was evaluated using a prismatic specimen of 160 x 40 x 40 mm, in accordance with [32].

These three tests were performed at 7, 28, and 56 days to assess the development of strength over time.

- Microstructural investigation of the mortar samples was performed after 56 days using Scanning Electron Microscopy (SEM). This method allows for a detailed examination of the morphology and phase distribution within the mortar, revealing crucial information about hydration products and porosity [33].

Fig. 5. Mortar specimens.

III. RESULTS

A. Setting Time

The setting time results, as can be seen in Figure 6, reveal the influence of GGBFS, RHA, calcined clay, and CDP on the setting behavior of mortars, compared to the control mix, M0, with 100% OPC, which had an initial setting time of 82 min and a final setting time of 235 min.

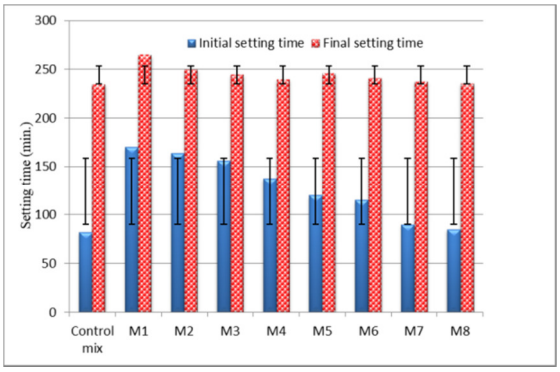

Fig. 6. Setting time results.

The presence of RHA increased the initial setting time, ranging from 138 to 170 min in the RHA-based mixes, M1-M4, representing an increase from 68.3% to 107.3% compared to the control mix. This delay is primarily due to the slower pozzolanic reaction of RHA, which reacts more gradually with calcium hydroxide than OPC. However, the addition of higher CDP content in these mixes (M3 and M4) slightly reduced the initial setting time, as CDP promotes the pozzolanic reaction, resulting in faster setting. Conversely, calcined clay-based mixes (M5-M8) experienced shorter setting delays, with initial setting times having ranged from 85 to 120 min, representing an increase from 3.6% to 46.3% compared to the M0. Calcined clay's higher reactivity compared to RHA, especially in the presence of CDP, accelerates the early hydration process, which explains the shorter setting times, as seen in M8, which had an initial setting time only 3.6% longer than the control mix. Similar trends were observed for the final setting times, with RHA-based mixes showing extended times from 240 to 265 min, up to 12.76% longer than M0, due to the slower formation of calcium silicate hydrates (C-S-H). On the other hand, calcined clay-based mixes had final setting times from 236 to 246 min, with M8 having achieved a final setting time 0.42% more than the M0, reflecting the accelerated C-S-H formation due to the enhanced reactivity of calcined clay and CDP. These results suggest that while RHA significantly prolongs both initial and final setting times due to its slower pozzolanic activity, calcined clay, especially when combined with CDP, offers a more reactive alternative that reduces setting times, obtaining values closer to those of the control mix.

B. Flowability

The flow table test was deployed to measure the flowability of the mortars. The results exhibited the influence of GGBFS, RHA, calcined clay, and CDP, on the workability of the geopolymer mortars compared to the control mix (100% OPC), which exhibited the highest flow at 192 mm, as depicted in Figure 7. The RHA mixes (M1-M4) exhibited a reduction in flowability, ranging from 171 mm to 185 mm, representing a decrease from 3.6% to 10.9% compared to the control mix.

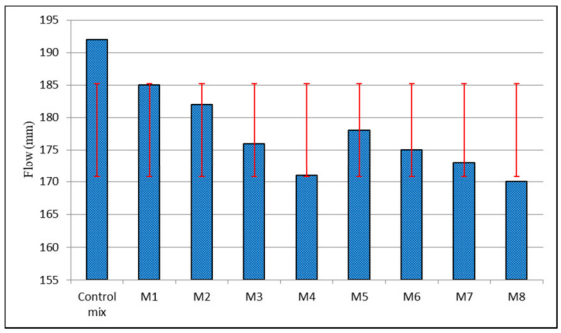

Fig. 7. Flowability of mortars.

This behavior is attributed to RHA's irregular particle shapes, which increase water demand and reduce flowability. Though CDP helps to slightly improve flowability by enhancing particle lubrication, the reduction remains significant due to RHA's high reactivity. Similarly, calcined clay mixes (M5-M8) exhibited flow values between 170 mm and 178 mm, with reductions from 7.3% to 11.5%. However, the impact on

flowability in these mixes was less severe compared to RHA, due to calcined clay's spherical particles that demand less water for dispersion. CDP also played a key role in enhancing flowability in both RHA and calcined clay mixes, with higher CDP content generally improving flow by reducing surface friction between the particles; however, not enough to match the flowability of the control mix. Overall the reductions in flowability, relative to the control mix, ranged from 3.6% to 11.5%.

C. Dry Unit Weight

Weights of mortar specimens at ages of 7, 28, and 56 days were measured in a dry state (oven-dried) and their dry unit weights were calculated. The dry unit weight results, as illustrated in Figure 8, show the impact of incorporating the GGBFS, RHA, calcined clay, and CDP on mortar density compared to M0, which exhibited the highest dry unit weights, namely 2.15 g/cm^3 at 7 days, 2.24 g/cm^3 at 28 days, and 2.3 g/cm^3 at 56 days.

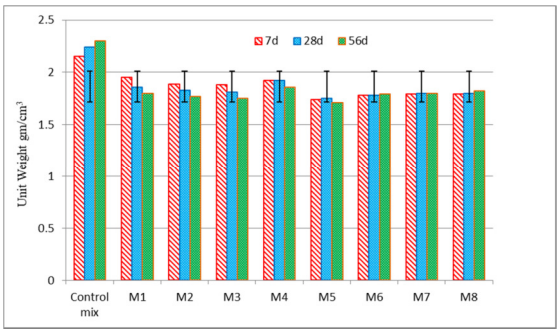

Fig. 8. Dry unit weight of mortars.

All geopolymer mixes showed reductions in dry unit weight, with RHA mixes having ranged from 1.88 to 1.95 g/cm^3 at 7 days, 1.81 to 1.92 g/cm^3 at 28 days, and 1.75 to 1.86 g/cm^3 at 56 days, reflecting decreases from 9.3% to 12.6% at 7 days, 14.3% to 17.0% at 28 days, and 19.1% to 21.7% at 56 days compared to the control mix. These reductions are largely due to RHA's porous nature and higher surface area, which increase air entrapment and lower overall density. In contrast, calcined clay-based mixes (M5-M8) exhibited slightly smaller reductions, with dry unit weights between 1.74 and 1.81 g/cm³ at 7 days, 1.75 and 1.82 g/cm^3 at 28 days, and 1.71 and 1.83 g/cm^3 at 56 days, corresponding to decreases from 15.8% to 18.8% at 7 days, 18.8% to 21.9% at 28 days, and 20.4% to 25.7% at 56 days. Calcined clay's higher reactivity allowed for better particle packing, having reduced the void content compared to the RHA mixes. The addition of CDP improved the dry unit weight slightly across both RHA and calcined clay mixes, as CDP enhances particle packing and reduces porosity. For instance, M4 (RHA-based) and M8 (calcined clay-based), both with the highest CDP content, showed higher dry unit weights compared to the mixes with lower CDP content.

D. Compressive Strength

Studying the results, outlined in Figure 9, of the compressive strength test for all examined mortars, it is observed that the compressive strength values of the mortar mixes containing RHA and calcined clay demonstrated significant differences compared to the control mix (100% OPC), with percentage comparisons having offered further clarity.

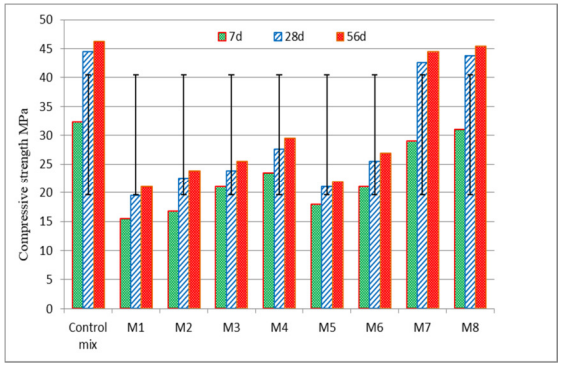

Fig. 9. Compressive strength of mortars at 7, 28, 56 days.

At 7 days, RHA-based mixes (M1–M4) achieved compressive strengths ranging from 15.5 MPa to 23.5 MPa, which were 52% to 27% lower than the control mix. This is owing to the slower reactivity of RHA, which limits early strength development despite its pozzolanic activity. In contrast, calcined clay mixes (M5–M8) demonstrated strengths between 18 MPa and 31 MPa, with M8 having reached 95.9% of the control's strength. By 28 days, the compressive strength of RHA mixes improved, but they remained 55% to 37% lower than the control mix (43.8 MPa). In contrast, the calcined clay mixtures and particularly M7 (42.6 MPa) and M8 (43.8 MPa), achieved 95.7% and 98.4% of the M0's strength, respectively. Calcined clay's rapid pozzolanic reactivity ensured higher strength at this stage, with denser microstructures having formed due to the ongoing C-S-H and C-A-H production [34]. At 56 days, the RHA mixes continued to gain strength but remained lower than both the control and calcined clay mixes, with M4 having reached 29.5 MPa, 38% lower than the control mix (47.5 MPa). However, calcined clay mixes, particularly M7 and M8, had compressive strength slightly less than the control mix by 3.6% and 1.7%, respectively. Overall, the comparison showed that the calcined clay-based mixes outperformed the RHA mixes at all stages, with calcined clay having achieved both higher early and long-term strength, particularly when combined with CDP [35].

E. Flexural Strengths

The results of the flexural strength test for all mixes, as displayed in Figure 10, show that M0 achieved the highest strength values at all curing ages, having reached 3.45 MPa at 7 days, 4.3 MPa at 28 days, and 4.75 MPa at 56 days. In comparison, geopolymer mixes exhibited reduced early strengths; nevertheless the performance gap diminished over time. For instance, at 7 days, the strength of the RHA mixes ranged from 1.8 to 2.3 MPa, representing a reduction from 33.3% to 47.8% compared to the control mix. Calcined clay mixes (M5 to M8) performed slightly better, with strengths ranging from 1.95 to 2.7 MPa, corresponding to reductions from 21.7% to 43.5% relative to the control mixture. At 28 days, similar trends were observed, with the RHA mixes

having demonstrated reductions from 41.9% to 53.5%, and the calcined clay mixes having exhibited reductions from 25.6% to 50%. After 56 days, the performance of geopolymer mixes improved significantly. For example, the mix with the highest CDP content, that is, 25% and 45% calcined clay (M8), achieved 3.8 MPa, which was only 20% lower than the control mix. In contrast, RHA-based mixes still lagged behind, with reductions from 41.1% to 51.6%.

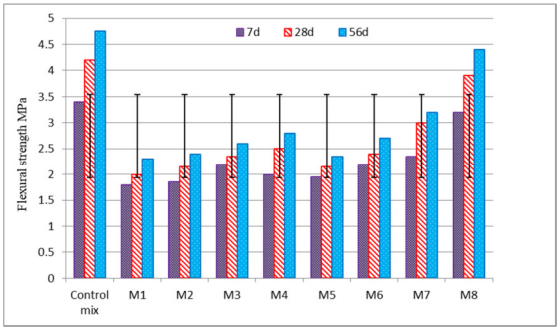

Fig. 10. Flexural strength of mortars at 7, 28, 56 days.

F. Microstructural Investigations

Figure 11 shows the SEM images of prepared mortars at the age of 56 days. In the control mix mortar (100% OPC), key hydration phases, including calcium silicate hydrate (C-S-H), calcium hydroxide $Ca(OH)_2$, and ettringite, define its microstructure. The amorphous C-S-H is the primary binding agent, filling voids and enhancing matrix cohesion to provide mechanical strength. The hexagonal, plate-like $Ca(OH)_2$, a by-product of tricalcium silicate (C_3S) and dicalcium silicate (C_2S) hydration, is structurally weaker than C-S-H and increases vulnerability to thermal and chemical deterioration. Needle-like ettringite, formed from tricalcium aluminate (C_3A) and gypsum, contributes to the initial setting time. In comparison, the geopolymer binder mortar with GGBFS, RHA, and CDP shows a cohesive microstructure, suggesting enhanced durability. In this study, GGBFS's spherical particles thickened the matrix through C-S-H formation, while the porous RHA clusters enhanced reactivity and bonding through geopolymerization. CDP promoted pozzolanic reactions with silica from RHA and GGBFS, having produced additional C-S-H and (C-A-S-H) that strengthened the matrix. Similarly, the geopolymer binder mortar containing GGBFS, calcined clay, and CDP displayed a densely packed structure with minimal porosity. Spherical GGBFS particles contributed to the C-S-H formation, while calcined clay introduced reactive aluminosilicates that generated sodium aluminosilicate hydrate gels, which enhanced durability. The increased CDP content (25%) maximized pozzolanic reactions with GGBFS and calcined clay, further forming C-S-H, thickening the matrix, and indicating high strength. In clay-based mortars, Stratlingite (CASH) improved compressive and flexural strength by reducing porosity and refining the pore structure, and Katoite (CAS) contributed by filling matrix voids, thus increasing density and mitigating cracking. Both phases enhanced durability, making the geopolymer mortar more robust and durable in aggressive environments [36].

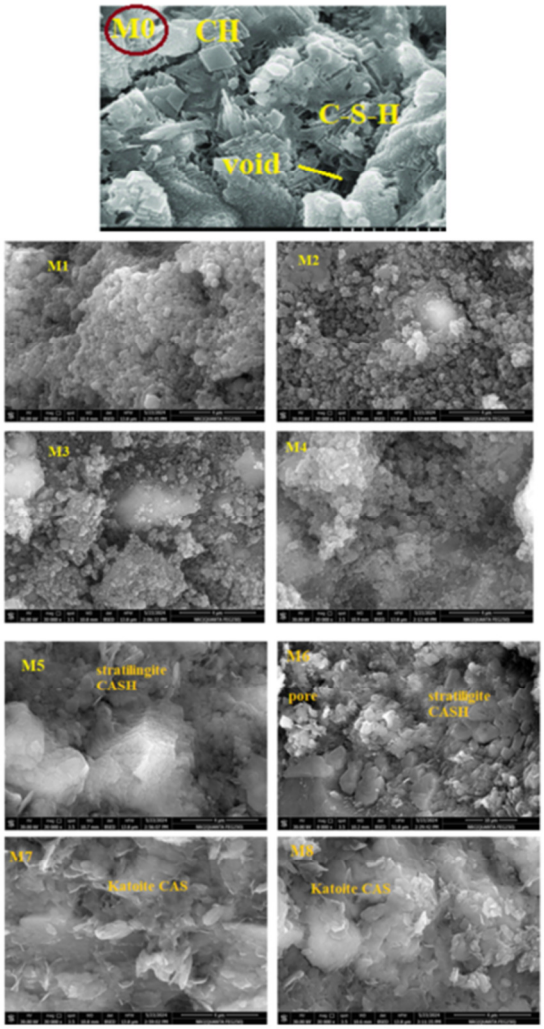

Fig. 11. SEM images of mortars at 56 days.

IV. CONCLUSION

This study examined the viability of geopolymer mortars composed of industrial or agriculture waste as sustainable alternatives to traditional Ordinary Portland cement (OPC). Having fully replaced natural sand with Recycled Concrete Aggregate and having utilized geopolymer binders composed of Ground Granulated Blast Furnace Slag (GGBFS), calcined clay, and Calcined Dolomite Powder (CDP), nine mortar mixes were prepared and tested to investigate their fresh and hardened properties. From the results, the following conclusions can be drawn:

Geopolymer mortar mixes M7 and M8 achieved compressive strengths of 42.6 MPa and 43.8 MPa, respectively, surpassing the standard compressive strength of OPC CEM I N at 28 days (42.5 MPa). This highlights the potential of tailored geopolymer formulations to meet or exceed conventional performance benchmarks. Furthermore, the microstructural analysis confirmed the formation of dense and robust binder matrices, particularly in mixtures containing calcined clay,

GGBFS, and CDP, contributing to improved strength and durability.

In comparison to previous studies, where geopolymer mortars often fell short of achieving compressive strengths comparable to OPC, this study demonstrates significant progress. For example, earlier works having utilized GGBFS and calcined materials typically reported compressive strengths around 70–90% of OPC strength [37], whereas the M7 and M8 mixes in this study achieved 98.4% and even exceeded the standard OPC strength. Similarly, the study's findings regarding the setting times provide new insights: mortars containing RHA exhibited significantly longer setting times compared to OPC, which may benefit applications requiring extended workability, while those with calcined clay offered a middle ground, balancing workability and setting characteristics.

This study also builds on the existing knowledge of geopolymer systems by emphasizing the synergistic role of calcined clay and CDP in forming robust matrices, filling a critical gap in previous studies that often focused solely on GGBFS as the primary contributor to strength [38]. The findings emphasize the potential of geopolymer mortars with RCA as a sustainable and technically viable alternative to OPC mortars. Mixtures M7 and M8, with their superior compressive strength and dense microstructures, stand out as practical replacements for traditional mortars in applications demanding comparable performance. The results affirm that appropriately selected and proportioned geopolymer binders can reduce reliance on natural resources and contribute to lower carbon emissions. Consequently, the adoption of such eco-friendly materials holds significant promise for advancing environmental friendly materials and mitigating environmental impacts associated with traditional cement manufacturing.

REFERENCES

[1] "Cement production global 2024," *Statista*. https://www.statista.com/statistics/1087115/global-cement-production-volume/.

[2] R. M. Andrew, "Global CO_2 emissions from cement production," *Earth System Science Data*, vol. 10, no. 1, pp. 195–217, Jan. 2018, https://doi.org/10.5194/essd-10-195-2018.

[3] N. Mahasenan, S. Smith, and K. Humphreys, "The cement industry and global climate change: current and potential future cement industry CO_2 emissions," in *6th international conference on greenhouse gas control technologies*, Kyoto, Japan, Oct. 2002, pp. 995–1000.

[4] M. S. Imbabi, C. Carrigan, and S. McKenna, "Trends and developments in green cement and concrete technology," *International Journal of Sustainable Built Environment*, vol. 1, no. 2, pp. 194–216, Dec. 2012, https://doi.org/10.1016/j.ijsbe.2013.05.001.

[5] E. Worrell, L. Price, N. Martin, C. Hendriks, and L. O. Meida, "Carbon Dioxide Emissions from the Global Cement Industry1," *Annual Review of Environment and Resources*, vol. 26, pp. 303–329, Nov. 2001, https://doi.org/10.1146/annurev.energy.26.1.303.

[6] J. L. Provis and J. S. J. van Deventer, "Alkali-activated materials," *Cement and Concrete Research*, vol. 114, pp. 40–48, Dec. 2018, https://doi.org/10.1016/j.cemconres.2017.02.009.

[7] P. Duxson, A. Fernández-Jiménez, J. L. Provis, G. C. Lukey, A. Palomo, and J. S. J. van Deventer, "Geopolymer technology: the current state of the art," *Journal of Materials Science*, vol. 42, no. 9, pp. 2917–2933, May 2007, https://doi.org/10.1007/s10853-006-0637-z.

[8] B. Ma *et al.*, "Assessing the viability of a high performance one-part geopolymer made from fly ash and GGBS at ambient temperature," *Journal of Building Engineering*, vol. 75, Sep. 2023, Art. no. 106978, https://doi.org/10.1016/j.jobe.2023.106978.

[9] S. Saha and C. Rajasekaran, "Enhancement of the properties of fly ash based geopolymer paste by incorporating ground granulated blast furnace slag," *Construction and Building Materials*, vol. 146, pp. 615–620, Aug. 2017, https://doi.org/10.1016/j.conbuildmat.2017.04.139.

[10] U. Zakira, K. Zheng, N. Xie, and B. Birgisson, "Development of high-strength geopolymers from red mud and blast furnace slag," *Journal of Cleaner Production*, vol. 383, Jan. 2023, Art. no. 135439, https://doi.org/10.1016/j.jclepro.2022.135439.

[11] M. Hongqiang *et al.*, "Study on the drying shrinkage of alkali-activated coal gangue-slag mortar and its mechanisms," *Construction and Building Materials*, vol. 225, pp. 204–213, Nov. 2019, https://doi.org/10.1016/j.conbuildmat.2019.07.258.

[12] M. Shaaban, "Properties of concrete with binary binder system of calcined dolomite powder and rice husk ash," *Heliyon*, vol. 7, no. 2, Feb. 2021, https://doi.org/10.1016/j.heliyon.2021.e06311.

[13] B. S. Thomas and R. C. Gupta, "A comprehensive review on the applications of waste tire rubber in cement concrete," *Renewable and Sustainable Energy Reviews*, vol. 54, pp. 1323–1333, Feb. 2016, https://doi.org/10.1016/j.rser.2015.10.092.

[14] S. H. Mohammed and N. M. Fawzi, "The Effect of the Utilization of Sustainable Materials on Some Mechanical Properties of Geopolymer Mortar," *Engineering, Technology & Applied Science Research*, vol. 14, no. 1, pp. 12464–12469, Feb. 2024, https://doi.org/10.48084/etasr.6378.

[15] W. G. Valencia-Saavedra, R. Mejía de Gutiérrez, and F. Puertas, "Performance of FA-based geopolymer concretes exposed to acetic and sulfuric acids," *Construction and Building Materials*, vol. 257, Oct. 2020, Art. no. 119503, https://doi.org/10.1016/j.conbuildmat.2020.119503.

[16] G. W. Kim, T. Oh, S. Kyun Lee, N. Banthia, and D. Y. Yoo, "Development of Ca-rich slag-based ultra-high-performance fiber-reinforced geopolymer concrete (UHP-FRGC): Effect of sand-to-binder ratio," *Construction and Building Materials*, vol. 370, Mar. 2023, Art. no. 130630, https://doi.org/10.1016/j.conbuildmat.2023.130630.

[17] M. S. Saif, M. O. R. El-Hariri, A. I. Sarie-Eldin, B. A. Tayeh, and M. F. Farag, "Impact of Ca+ content and curing condition on durability performance of metakaolin-based geopolymer mortars," *Case Studies in Construction Materials*, vol. 16, Jun. 2022, Art. no. e00922, https://doi.org/10.1016/j.cscm.2022.e00922.

[18] G. Kastiukas, S. Ruan, S. Liang, and X. Zhou, "Development of precast geopolymer concrete via oven and microwave radiation curing with an environmental assessment," *Journal of Cleaner Production*, vol. 255, May 2020, Art. no. 120290, https://doi.org/10.1016/j.jclepro.2020.120290.

[19] F. K. Alqahtani, K. Rashid, I. Zafar, and M. Iqbal Khan, "Assessment of morphological characteristics and physico-mechanical properties of geopolymer green foam lightweight aggregate formulated by microwave irradiation," *Journal of Building Engineering*, vol. 35, Mar. 2021, Art. no. 102081, https://doi.org/10.1016/j.jobe.2020.102081.

[20] M.-H. Nofalah, P. Ghadir, H. Hasanzadehshooiili, M. Aminpour, A. A. Javadi, and M. Nazem, "Effects of binder proportion and curing condition on the mechanical characteristics of volcanic ash- and slag-based geopolymer mortars; machine learning integrated experimental study," *Construction and Building Materials*, vol. 395, Sep. 2023, Art. no. 132330, https://doi.org/10.1016/j.conbuildmat.2023.132330.

[21] Y. Luo, S. H. Li, K. M. Klima, H. J. H. Brouwers, and Q. Yu, "Degradation mechanism of hybrid fly ash/slag based geopolymers exposed to elevated temperatures," *Cement and Concrete Research*, vol. 151, Jan. 2022, Art. no. 106649, https://doi.org/10.1016/j.cemconres.2021.106649.

[22] Z. Hu, M. Wyrzykowski, and P. Lura, "Estimation of reaction kinetics of geopolymers at early ages," *Cement and Concrete Research*, vol. 129, Mar. 2020, Art. no. 105971, https://doi.org/10.1016/j.cemconres.2020.105971.

[23] D. L. Y. Kong and J. G. Sanjayan, "Effect of elevated temperatures on geopolymer paste, mortar and concrete," *Cement and Concrete Research*, vol. 40, no. 2, pp. 334–339, Feb. 2010, https://doi.org/10.1016/j.cemconres.2009.10.017.

[24] Z. Dong, H. Ma, W. Feng, Y. Nie, and H. Shi, "Achieving superior high-strength geopolymer via the synergistic effect of traditional oven curing and microwave curing," *Construction and Building Materials*, vol. 357, Nov. 2022, Art. no. 129406, https://doi.org/10.1016/j.conbuildmat.2022.129406.

[25] Subcommittee C09.20, *ASTM C136/C136M-19 : Standard Test Method for Sieve Analysis of Fine and Coarse Aggregates*. West Conshohocken, PA, USA: ASTM International, 2020.

[26] Subcommittee C01.10, *ASTM C150/C150M-19a: Standard Specification for Portland Cement*. West Conshohocken, PA, USA: ASTM International, 2020.

[27] Subcommittee C09.40, *ASTM C1602/C1602M-18: Standard Specification for Mixing Water Used in the Production of Hydraulic Cement Concrete*. West Conshohocken, PA, USA: ASTM International, 2022.

[28] Subcommittee C01.30, *ASTM C191-21: Standard Test Methods for Time of Setting of Hydraulic Cement by Vicat Needle*. West Conshohocken, PA, USA: ASTM International, 2021.

[29] Subcommittee C01.22, *ASTM C1437-20: Standard Test Method for Flow of Hydraulic Cement Mortar*. West Conshohocken, PA, USA: ASTM International, 2020.

[30] Subcommittee C09.60, *ASTM C138/C138M-16a: Standard Test Method for Density (Unit Weight), Yield, and Air Content (Gravimetric) of Concrete*. West Conshohocken, PA, USA: ASTM International, 2017.

[31] Subcommittee C01.27, *ASTM C109/C109M-20b: Standard Test Method for Compressive Strength of Hydraulic Cement Mortars (Using 2-in. or [50 mm] Cube Specimens)*. West Conshohocken, PA, USA: ASTM International, 2021.

[32] Subcommittee C01.27, *ASTM C348-20: Standard Test Method for Flexural Strength of Hydraulic-Cement Mortars*. West Conshohocken, PA, USA: ASTM International, 2021.

[33] K. L. Scrivener and R. J. Kirkpatrick, "Innovation in use and research on cementitious material," *Cement and Concrete Research*, vol. 38, no. 2, pp. 128–136, Feb. 2008, https://doi.org/10.1016/j.cemconres.2007.09.025.

[34] R. Fernandez, F. Martirena, and K. L. Scrivener, "The origin of the pozzolanic activity of calcined clay minerals: A comparison between kaolinite, illite and montmorillonite," *Cement and Concrete Research*, vol. 41, no. 1, pp. 113–122, Jan. 2011, https://doi.org/10.1016/j.cemconres.2010.09.013.

[35] S. Rukzon and P. Chindaprasirt, "Utilization of bagasse ash in high-strength concrete," *Materials & Design*, vol. 34, pp. 45–50, Feb. 2012, https://doi.org/10.1016/j.matdes.2011.07.045.

[36] K. L. Scrivener, V. M. John, and E. M. Gartner, "Eco-efficient cements: Potential economically viable solutions for a low-CO_2 cement-based materials industry," *Cement and Concrete Research*, vol. 114, pp. 2–26, Dec. 2018, https://doi.org/10.1016/j.cemconres.2018.03.015.

[37] P. Nath and P. K. Sarker, "Effect of GGBFS on setting, workability and early strength properties of fly ash geopolymer concrete cured in ambient condition," *Construction and Building Materials*, vol. 66, pp. 163–171, Sep. 2014, https://doi.org/10.1016/j.conbuildmat.2014.05.080.

[38] H. Xu and J. S. J. Van Deventer, "The geopolymerisation of alumino-silicate minerals," *International Journal of Mineral Processing*, vol. 59, no. 3, pp. 247–266, Jun. 2000, https://doi.org/10.1016/S0301-7516(99)00074-5.